Statistical thermodynamics of molecular organization in mixed micelles and bilayers

I. Szleifer and A. Ben-Shaul
Department of Physical Chemistry, and The Fritz Haber Molecular Dynamics Research Center, The Hebrew University, Jerusalem, 91904 Israel

W. M. Gelbart
Department of Chemistry and Biochemistry, University of California, Los Angeles, Los Angeles, California 90024

(Received 29 December 1986; accepted 12 March 1987)

The conformational and thermodynamic characteristics of molecular organization in *mixed* amphiphilic aggregates of different compositions and geometries are analyzed theoretically. Our mean-field theory of chain conformational statistics in micelles and bilayer membranes is extended from pure to mixed aggregates, without invoking any additional assumptions or adjustable parameters. We consider specifically binary aggregates comprised of long-chain and short-chain surfactants, packed in spherical micelles, cylindrical rods, and planar bilayers. Numerical results are presented for mixtures of 11- and 5-carbon chain amphiphiles. The probability distribution functions (pdfs) of the (different types of) chains are determined by minimizing the conformational free energy, subject to packing constraints which reflect the segment density distribution within the hydrophobic core. In order to analyze the relative thermodynamic stabilities of mixed aggregates of different compositions (long/short chain ratios) and different geometries, the aggregate's free energy is expressed as a sum of conformational, surface, and mixing contributions. The conformational free energy is determined by the pdfs of the chains and the surface term is modeled in terms of the "opposing forces" operative at the hydrocarbon–water interface. An interesting coupling between these terms arises from the special geometric (surface/volume) limitations associated with packing short and long chains in a given ratio within a given aggregate. In particular, it is found that the minimal area per surfactant head group in a mixed spherical micelle is significantly lower than that in a pure micelle (similarly, though less drastically so, for cylindrical micelles). The most important qualitative conclusion of our thermodynamic analysis is that the preferred aggregation geometry may vary with composition. For example, we find that under certain conditions (areas per head group, chain lengths) the preferred micellar geometry of pure long or short-chain aggregates is that of a planar bilayer, whereas at intermediate compositions spherical micelles are more stable. Our analysis of chain conformational properties provides quantitative information on the extent of long (or short) chain distortion attendant upon chain mixing. For example, the results for bond order parameter profiles and segment density distributions reveal enhanced stretching of the long chain towards the central regions of the hydrophophic core as the fraction of short chains is increased.

I. INTRODUCTION

Most amphiphilic aggregates of interest comprise more than one component. Biological membranes containing several lipids, as well as other molecules (e.g., cholesterol), are perhaps the best known examples. Other familiar systems are mixed micelles of various kinds, and surfactant–cosurfactant (alcohol) films in microemulsions.[1–4] Similarly, all micelles and vesicles incorporating solubilized species are mixed aggregates. In addition, as far as molecular organization in amphiphilic aggregates is concerned, some systems should be treated as mixed aggregates although they only contain one chemical component. This refers in particular to lipid bilayers in which the two acyl chains of the constituent molecules are not entirely equivalent, even if their chain lengths are the same (of course this holds as well for asymmetric lipids). Furthermore, the hydrophobic cores of one component amphiphilic bilayers, both planar and vesicular, are packed by two (chemically identical but "topologically" different) types of chains, namely, those originating from the two ("inner" and "outer") hydrocarbon–water interfaces.

Thermodynamic characteristics such as phase behavior and critical micelle concentration have been extensively and thoroughly studied for numerous and diverse ternary (and higher order) micellar solutions.[5,6] Also, the global symmetries of the aggregates in the various macroscopic phases are usually well known (e.g., cylindrical rod-like micelles in hexagonal phases, bilayers in lamellar phases, etc.). On the other hand, much less information is available about the microscopic structure and molecular organization of the aggregates, which are intimately related to their thermodynamic stability and macroscopic (e.g., elastic) properties. For example, it is well known that incorporation of bile-salts into lecithin vesicles leads, at high bile-salt concentration, to the

 0021-9606/87/127094-16$02.10

formation of mixed lecithin/bile salt micelles.[7–9] Several models have been suggested for the structure of these micelles, but no direct structural evidence to support them is available. Similarly, it is known that the addition of alcohols to concentrated ionic surfactant solutions induces a transition from an hexagonal to a lamellar phase[5] but the microscopic organization of the two amphiphilic components in the aggregates is not well understood. Similarly unclear is the location of short chain alcohols in small micelles (which varies with alcohol content).[10]

We have recently presented a statistical thermodynamic ("mean-field" or "single-chain") theory for chain conformational statistics and thermodynamics in micellar aggregates of different geometries.[11–13] So far the theory has been applied to pure aggregates, and the results pertaining to measured quantities (e.g., bond order parameters) show good agreement with available experimental data[14,15] (as well as with large scale computer simulations[16–18]). In this paper we extend the theory and apply it to mixed aggregates. More specifically, we consider binary aggregates comprised of mixtures of long chain and short chain surfactants in various proportions. Our major objective is to study the changes in chain conformational properties and free energies associated with changes in the aggregate's composition and packing geometry (e.g., spherical micelles vs planar bilayers). In analyzing the thermodynamic stability of the aggregates we include, in addition to the chain (hydrophobic core) contribution to the free energy, the more familiar terms associated with "opposing forces" operative at the micelle–water interface.[1,19]

Wherever possible our calculations will be compared with the few available experimental results on chain conformational properties (such as bond order parameters) in mixed aggregates.[20–23] But for the most part our conclusions concern more qualitative considerations. A particular phenomenon which we address is the observation by Charvolin and Mely that mixtures of $C_{10}K$ and $C_{18}K$ (potassium soap) chains form bilayers (in lamellar phases) in the two narrow composition regimes corresponding to low concentrations of one soap in the other.[24] At intermediate compositions however the amphiphiles form a stable isotropic, presumably cubic, phase. Mixtures of molecules whose chains are less disparate, e.g., $C_{18}K$ and $C_{14}K$, form stable bilayers at all compositions.

Mixed aggregates of similar size chains (e.g., C_{10} and C_8) have been considered theoretically (and compared with experiments[23]) by Gruen.[25] As previously pointed out, his pdf (probability distribution function) of chain conformations for pure aggregates and the one which we have derived are basically identical. (The differences between the two approaches appear mainly in the evaluation of the pdf parameters.[12]) However, in order to apply his model to mixed aggregates, Gruen has modified his pdf by introducing adjustable optimization parameters which are determined by fitting to experimental data.[25(b)] On the other hand, as will be shown in the next section, the extension of our theory to mixed aggregates is a simple consequence of modified chain packing constraints and does not involve any new parameters.

II. THEORY

The derivation of the pdf of chain conformations presented below is based on minimizing the conformational (packing) free energy of the hydrocarbon chains ("tails") constituting the hydrophobic cores of amphiphilic aggregates. Using this pdf we can calculate both structural and thermodynamic properties of the chains. The conformational free energy of the amphiphiles is one, but not the only, important contribution to the aggregate's total free energy. In this paper we are interested in the conformational statistics of the hydrocarbon chains in mixed aggregates as well as in the role of chain packing in determining the thermodynamic stability of these aggregates. Since the stability of micellar aggregates is governed by the sum of several contributions to their total free energy we open this section with a brief discussion of these terms.

The free energy of a micellar solution is naturally divided into "external" and "internal" parts. The external part incorporates terms accounting for the translational ("entropy of mixing") and rotational motions of the aggregates (regarded as nearly rigid particles) as well as intermicelle interactions. The internal part includes all contributions to the free energy (standard chemical potential) of an isolated, fixed-in-space, aggregate. The internal free energy depends on interamphiphile interactions and conformational energies and entropies, as well as kinetic (translational/rotational) contributions associated with the motion of the molecules within the aggregate.

Micellar solutions can respond to changes in external variables such as total amphiphile concentration, temperature, or ionic strength by changes in aggregation geometry, e.g., sodium dodecyl sulfate (SDS) micelles grow from spheres to cylindrical rods upon increase in surfactant concentration.[19,26,27] This reflects a decrease in the internal free energy of the micelles (due to favorable packing of the surfactant in cylindrical geometry), which exceeds the increase in external free energy ("entropy of mixing") loss associated with surfactant organization in larger, rod-like, micelles. This unique property of micellar systems implies an intrinsic coupling between internal and external free energies, corresponding to the fact that micellar aggregates do not maintain their integrity. Thus, in determining the relative thermodynamic stability of a given micellar phase one has to consider both the internal and external free energy contributions. Yet, each of these may be calculated separately. In this paper we shall focus attention on the *internal* free energy of mixed aggregates and its dependence on micellar geometry and chemical composition. It should be borne in mind, however, that conclusions regarding the relative stability of different macroscopic phases should include the external free energy as well.

The internal free energy (standard chemical potential) of an amphiphilic aggregate involves both kinetic (momentum) and configurational (coordinate) contributions. It has been argued elsewhere that the momentum contributions to the total free energy are independent of the aggregates' size and shape distributions, and, therefore, play no role in determining the relative stability of different aggregates.[19(c)]

Based on this notion the following discussion is limited to the configurational part of the internal (Helmholtz) free energy. We shall denote this quantity by A.

The aggregate's free energy A is commonly separated into "surface" and "core" terms A_S and A_C.[1,11–13,19] This separation is largely based on the standard picture of micellar aggregates which depicts them as particles with a liquid-like hydrophobic core (comprised by the amphiphiles' hydrocarbon tails) surrounded by an interfacial (hydrocarbon–water) region containing the hydrophilic heads.[1,6,19,28] The separation $A = A_S + A_C$ implies that the interactions at the interfacial regions are independent of those (between the tails) responsible for the cohesiveness of the hydrophic core. We have discussed this separation from a statistical-thermodynamic point of view and concluded that it is a most reasonable approximation and, hence, adopt it in the forthcoming discussion.[11–13] Since we are dealing with mixed aggregates we add to A_S and A_C a term A_M, accounting for the "mixing" free energy of the different amphiphilic components, i.e., we write

$$A = A_C + A_S + A_M. \tag{1}$$

Most of the discussion below will be devoted to the core term A_C which depends on the conformational properties of the hydrocarbon tails in mixed aggregates. As noted in Sec. I, these have not been satisfactorily studied to date. Our treatment of the surface term will be on a phenomenological level, in terms of "opposing forces."[1,19] The inclusion of A_S is mainly important for assessing the relative stabilities of different aggregation geometries as a function of amphiphile composition. In the derivation below we shall consider binary aggregates comprised of two single-chain amphiphiles of the type h_K–$(CH_2)_{n_K-1}$–CH_3 ($K = A,B$). Here h_K denotes the hydrophilic head group of amphiphile K and n_K is its tail length. Application of the theory to more than two components or different types of amphiphiles, e.g., double chain lipids or partly unsaturated chains is (at least in principle) straightforward. The calculations presented in Sec. III apply to three basic micellar geometries: spherical micelles, cylindrical (rod-like) aggregates, and planar bilayers. Again, the treatment of other structures (e.g., vesicles) is analogous.

A. Core free energy and chain pdf

Following the separation of tail and head contributions in Eq. (1), the hydrophobic core may be treated as a system of densely packed hydrocarbon chains, all originating from the narrow interfacial region. The head groups of the A and B amphiphiles are assumed to be randomly distributed over the interface. Let a_j denote the chain conformation of amphiphile j of type A, $j = 1,2,...,N_A$. Similarly, b_l denotes the conformation of the lth chain of type B, $l = 1,2,...,N_B$. As in previous papers the term conformation is used to specify both the bond (*trans/gauche*) sequence of the chain and its overall orientation relative to the hydrocarbon–water interface.[11–13]

Using $P(\mathbf{a},\mathbf{b}) = P(a_1,...,a_{N_A},b_1,...,b_{N_B})$ to denote the many-chain pdf in the hydrophobic core, the conformational free energy ("per chain") is given by

$$A_C = \frac{1}{N}\left\{\sum_{\mathbf{a},\mathbf{b}} P(\mathbf{a},\mathbf{b})E(\mathbf{a},\mathbf{b}) + kT\sum_{\mathbf{a},\mathbf{b}} P(\mathbf{a},\mathbf{b})\ln P(\mathbf{a},\mathbf{b})\right\} \tag{2a}$$

$$= E_C - TS_C \tag{2b}$$

with the first and second terms representing the energetic and entropic contributions to A_C, respectively. $E(\mathbf{a},\mathbf{b})$ is the energy of the many-chain configuration and $N = N_A + N_B$.

Most of the currently measurable chain conformational properties, e.g., bond order parameter profiles or segment spatial distributions, are single chain properties, i.e., they are determined by the singlet distribution functions, $P_A(a)$ and $P_B(b)$ ($a = a_j, j = 1,...,N_A$, etc.). These pdf's are rigorously defined by

$$P_A(a) = \sum_{a_2,...,a_{N_A}} \sum_{b_1,...,b_{N_B}} P(a = a_1,a_2,...,a_{N_A},b_1,...b_{N_B}) \tag{3}$$

with an analogous definition for $P_B(b)$. We assume that all A chains are subject to the same boundary conditions, so that $P_A(a_j)$ is independent of j. Similarly, all B chains are equivalent. In other words, we consider aggregates, or portions thereof, with a uniform and well defined geometry, e.g., spherical micelles, portions of planar bilayers, etc.

In previous papers we have shown that the singlet pdf (for pure aggregates) can be derived by two alternative approaches.[11] One derivation begins with Eq. (3) and consists of appropriate expansion of the many-chain configurational partition function. A shorter, though less informative derivation (in terms of treating the interchain potential), is based on a "mean-field" decomposition of A_C corresponding to a factorization of the many-chain pdf into a product of singlet distribution functions. We shall follow here this second derivation, emphasizing the modifications in packing criteria implied by the presence of two types of chains. It should be emphasized that the singlet pdf's and single chain properties derived by the mean-field approach are in excellent agreement with those obtained from many-chain molecular dynamics simulations.[11,25,26] The theoretical reasoning underlying this fact is discussed in more detail elsewhere.[11–13]

Our theory requires specification of the chain segment (monomer) density distribution within the hydrophobic core. We usually assume, in accord with most experimental observations that the monomer density is uniform and liquid-like throughout the core.[28,29] [We do allow, however, for lower densities in the interfacial region, thereby (indirectly) accounting for surface roughness,[12] see Sec. III.] For aggregates with high symmetry, e.g., spheres, bilayers, and cylinders, the local monomer density $\rho(r)$ depends only on the distance r from the hydrocarbon–water interface, or equivalently from the aggregate's center (or midplane in bilayers, etc.). We shall refer to $\rho(r)$ as the "density profile." The density profile and the aggregation geometry G impose packing constraints on the pdf of chain conformations. To formulate these constraints we first need a more quantitative characterization of the micellar geometry G. This is conveniently achieved (mainly for computational purposes) by dividing the hydrophobic core into, say L imaginary layers concentric (parallel) to the interface,[11–13] see Fig. 1. Al-

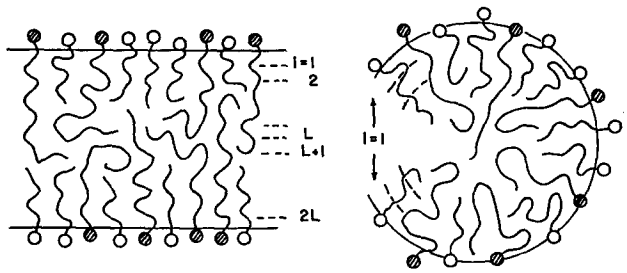

FIG. 1. Schematic representation of a mixed planar bilayer (left) and spherical or cylindrical micelle (right). The hydrophobic core is divided into L imaginary layers ($2L$ in the case of a bilayer). Note that the inner regions of the aggregate can be reached only by the long chains.

though other choices are possible we simply take all layers to have the same width, d. The layers are denoted by $i = 1,...,L$ starting from the interface towards the center of the core. In planar bilayers we divide the core into $2L$ layers, i.e., $i = 1$ and $2L$ are the layers at the two interfaces.

The micellar geometry G is specified by $\{M_i\}$, where M_i is the volume of layer i. Thus, for example, $M_i \propto (L-i+1)^D - (L-i)^D \sim (L-i)^{D-1}$ with $D = 1,2$ and 3 for planar, cylindrical and spherical aggregates, respectively. (Of course, in the calculations the M_is are evaluated exactly.) We also define $m_i \equiv M_i/N$ which may be referred to as the average volume available per chain in layer i where, as before, $N = N_A + N_B$. (In bilayers N is the number of chains anchored to one of the interfaces.) With ρ_i denoting the monomer density in layer i, $\rho_i M_i$ is the total number of monomers in this layer,and $\rho_i m_i$ is the average number of monomers per chain (of either A or B chains) in this layer. Now let $\phi_{A,i}(a_j)$ denote the number of monomers of the jth A chain which are in layer i when the chain has conformation a_j. $\phi_{B,i}(b_l)$ is the corresponding quantity for the l th B chain. Clearly,

$$\sum_{\mathbf{a}}\sum_{\mathbf{b}} P(\mathbf{a},\mathbf{b})\left\{\sum_{j=1}^{N_A}\phi_{A,i}(a_j)+\sum_{l=1}^{N_B}\phi_{B,i}(b_l)\right\}=\rho_i M_i. \quad (4)$$

Using Eq. (3) and noting the equivalence of all the A chains and all the B chains it is easily verified that

$$X_A\sum_a P_A(a)\phi_{A,i}(a)+X_B\sum_b P_B(b)\phi_{B,i}(b)=\rho_i m_i \quad (5a)$$

or, in slightly different notation

$$\langle\phi_i\rangle = X_A\langle\phi_{A,i}\rangle + X_B\langle\phi_{B,i}\rangle = \rho_i m_i, \quad (5b)$$

where $X_A = N_A/N$ and $X_B = N_B/N = 1 - X_A$, are the mole fractions of A and B chains in the aggregate.

A few "technical" remarks:

(i) The monomers in our problem are the CH_2 segments of the hydrocarbon tails. The volume (in bulk liquid hydrocarbon) taken up by a terminal CH_3 group is approximately twice (~ 54 Å^3) that of a CH_2 group (~ 27 Å^3).[1] Thus, in our calculations a CH_3 group counts as two monomers.

(ii) In planar bilayers the central regions of the hydrophobic core (near the midplane) can be reached by chains originating in either one of the two interfaces. Thus, even in one component aggregates the core volume is filled up by two types of chains. Accordingly, for binary aggregates $\langle\phi_i\rangle$ is actually a sum of four rather than two terms. For symmetric bilayers (i.e., with the X_A identical for both interfaces) the modification of Eq. (5) is straightforward; namely, instead of $\langle\phi_{A,i}\rangle$ we should write $\langle\phi_{A,i}\rangle + \langle\bar{\phi}_{A,i}\rangle$ where $\langle\phi_{A,i}\rangle$ and $\langle\bar{\phi}_{A,i}\rangle$ represent the contributions to the monomer density from chains anchored to opposite interfaces. Clearly $\phi_{A,i}(a) = \bar{\phi}_{A,2L-i+1}(a)$, by symmetry, and similarly for B chains. We shall keep using the simple form (5) but it should be stressed that in our calculations for bilayers the existence of two interfaces is explicitly taken into account.

(iii) Uniform segment density in the core corresponds to $\rho_i = $ constant for all layers i. In some cases (see Sec. III), we allow for lower monomer density near the water–hydrocarbon interface (i.e., in layers with small i). For instance, in spherical micelles we take $\rho_1 < \rho_2 < \rho_3 = \rho_4 = ... \rho_L$, etc.[12]

(iv) If the monomer density is liquid-like, $\rho_i = \rho_l = 1/\nu$ where $\nu(\sim 27$ Å$^2)$ is the "specific volume" of a CH_2 segment. Note however that only relative densities, ρ_i/ρ_i' are important in our model, due to the existence of a conservation condition on the total number of monomers. Namely, since $\Sigma_i\langle\phi_{K,i}\rangle = n_K + 1 (n_k - 1$ is the number of CH_2 segments, and CH_3 segments count as two monomers), it follows from Eq. (5) that

$$X_A(n_A+1)+X_B(n_B+1)=\sum_{i=1}^{L}\rho_i m_i, \quad (6)$$

i.e., the ρ_i are linearly dependent.

(v) m_i's are proportional to the areas available per chain in layer i. In particular m_1, the volume per chain in the outermost (surface) layer, is proportional to a, the average area per chain, or head group, at the aggregate's surface; this quantity plays a central role in all theories of micelle structure.[1,19]

The mean-field approach to the derivation of the singlet pdfs consists of two (related) approximations. First, the many-chain pdf is expressed as a product of singlet pdfs

$$P(\mathbf{a},\mathbf{b}) = \prod_{j=1}^{N_A} P_A(a_j)\prod_{l=1}^{N_B} P_B(b_l). \quad (7)$$

Second, the total energy of a many-chain configuration is written as a sum of single-chain energies

$$E(\mathbf{a},\mathbf{b}) = \sum_{j=1}^{N_A}\epsilon_A(a_j)+\sum_{l=1}^{N_B}\epsilon_B(b_l). \quad (8)$$

From Eqs. (2), (7), and (8), and noting the equivalence of the N_A A chains and of the N_B B chains, we find

$$A_C = X_A\left[\sum_a P_A(a)\epsilon_A(a) + kT\sum_a P_A(a)\ln P_A(a)\right] + X_B\left[\sum_b P_B(b)\epsilon_B(b) + kT\sum_b P_B(b)\ln P_B(b)\right] \quad (9)$$

or,

$$A_C = X_A A_{C,A} + X_B A_{C,B} \tag{10}$$

with

$$A_{C,A} = \sum_a P_A(a)\epsilon_A(a) + kT\sum_a P_A(a)\ln P_A(a)$$
$$= E_{C,A} - TS_{C,A}, \tag{11}$$

where $E_{C,A} = \langle \epsilon_A \rangle$ and $S_{C,A}$ are the ("partial molar") energy and entropy of A chains. Similar definitions apply for B chains. Note that $A_{C,A}$ depends on composition X_A.

The configurational energy, cf. Eq. (8), is the sum of internal (*trans/gauche*) chain energies and interchain potentials. The interaction energy may be separated (to a good approximation) into repulsive and attractive contributions $U = U_r + U_a$ representing the corresponding separation of the pairwise interchain potentials. The attractive (van der Waals) interactions are responsible for the cohesiveness of the aggregate, but as in liquids,[30] play a minor role in determining the molecular organization (packing) of chains. Since the density of the core is essentially uniform, the attractive potential energy is nearly independent of chain configuration [**a**,**b**], and may be regarded (as in the familiar van der Waals picture) as a constant attractive background depending only on the monomer density. This contribution to E can be expressed as $U_a = (N_A n_A + N_B n_B)g$ where g is the average ("mean-field") attractive potential per monomer in the core: taking the bulk liquid hydrocarbon as the reference for measuring g we clearly have $g \equiv 0$.

The repulsive potentials between chain segments dominate chain organization in the core. Expressed as sums of hard core repulsive potentials it follows that $U_r(\mathbf{a},\mathbf{b})$ is either infinity or zero, depending on whether any two monomers do, or do not, "overlap" in space: $U_r = \infty$ for all forbidden (overlapping) configurations for which $P(\mathbf{a},\mathbf{b}) = 0$, and $U_r = 0$ for all allowed configurations. In our theory the discrimination between allowed and forbidden configuration is taken care of (approximately, of course) by the packing constraints (4) or (5). The formal implication of this procedure is that we impose Eq. (4) on $P(\mathbf{a},\mathbf{b})$ and set $U_r \equiv 0$. Now, since both $U_r = 0$ and $U_a = \text{const} = 0$, the configurational energy in Eq. (8) is simply a sum of *internal* chain energies. Thus, $\epsilon_A(a)$ is determined only by the bond sequence characterizing a. In our calculations the chains are treated in the rotational-isomeric-state (RIS) model scheme[31], so that $\epsilon_A(a) = k_g(a)e_g$ where $k_g(a)$ is the number of *gauche* bonds along the chain and e_g (~ 500 cal mol) is the *gauche* energy. Self-crossing chain conformations and those involving g^+g^- or/and g^-g^+ bond pairs ("pentane effect") are excluded [$\epsilon(a) \equiv \infty$].

There are many pdfs which satisfy the packing constraints (4). Similarly, there are many (actually an infinity of) pdfs of the type (7) which satisfy Eq. (5). The "best" (mean-field) distribution is determined by requiring that it should not only satisfy the packing constraints (5) but also minimize the free energy functional (9). The variational (minimization) procedure is standard (using the Lagrange multipliers method). In the present case we obtain the following explicit expressions for both $P_A(a)$ and $P_B(b)$:

$$P_A(a) = \frac{1}{z_A}\exp\left[-\beta\epsilon_A(a) - \beta\sum_{i=1}^{L}\pi_i\phi_i(a)\right]$$
$$= \frac{1}{z_A}\omega_A(a)\prod_{i=1}^{L}\alpha_i^{\phi_{i,A}(a)}, \tag{12}$$

$$P_B(b) = \frac{1}{z_B}\exp\left[\beta\epsilon_B(b) - \beta\sum_{i=1}^{L}\pi_i\phi_i(b)\right]$$
$$= \frac{1}{z_B}\omega_B(b)\prod_{i=1}^{L}\alpha_i^{\phi_{i,B}(b)}, \tag{13}$$

where z_A and z_B are the (single-chain) partition functions (normalization constants) for A and B, respectively. $\omega_A(a) \equiv \exp[-\beta\epsilon_A(a)]$, etc. $\lambda_i \equiv \beta\pi_i \equiv -\ln\alpha_i$ are the Lagrange multipliers conjugate to the packing constraints (5). They are determined (formally and numerically) by substituting $P_A(a)$ and $P_B(b)$ from Eqs. (12) and (13) into Eq. (5) and solving the resulting set of nonlinear equations for the π_is (or α_is). Because of the conservation condition (6) only $L-1$ of the L equations are independent; as has been shown elsewhere, this implies that one of the π_is can be chosen arbitrarily.[11] We usually set $\pi_L = 0$, but other choices are possible.

It has been shown previously[11] that the π_is are, dimensionally, and *physically*, the lateral pressures in the imaginary layers i. In other words, they are related to the free energy changes (derivatives) associated with squeezing a chain (constrained only by impenetrability of the interface) into the volume available to it in layer i. It should be noted that the π_i's (α_i's) appearing in both $P_A(a)$ and $P_B(b)$ *are the same*. Clearly, as is obvious from the packing constraints (5), with the aid of which the π_is are determined, the π_is *depend both on the geometry of the aggregate* (i.e., on $\{\rho_i m_i\}$) *and on its composition* ($X_A, X_B = 1 - X_A$).

With the aid of $P_A(a)$ and $P_B(b)$ we can calculate any desired conformational property of chains A or B, (e.g., bond order profiles). Of course, since the π_i's and hence the singlet pdfs are dependent on the geometry and the composition of the aggregate, so also are the conformational properties.

Substituting Eqs. (12) and (13) back into Eq. (9) we calculate the aggregates free energy, A_C and similarly, $A_{C,A}, S_{C,A}, E_{C,A}, S_C$, etc. Note, for example,that the conformational free energy can be expressed as

$$A_C = -X_A\left\{kT\ln z_A + \sum_i \pi_i\langle\phi_{i,A}\rangle\right\}$$
$$-X_B\left[kT\ln z_B + \sum_i \pi_i\langle\phi_{i,B}\rangle\right]$$
$$= -X_A kT\ln z_A - X_B kT\ln z_B - \sum_i \pi_i\rho_i m_i, \tag{14}$$

where in the second line of Eq. (14) we have used Eq. (5b). It has been remarked earlier that one of the π_is may be chosen arbitrarily. Equivalently, the π_is are defined up to an arbitrary additive constant. This constant could also be chosen such that the last term (the sum) in Eq. (14) is zero, thereby simplifying the expression of A_C. (Of course, this is equivalent to absorbing the sum into $\ln z_A$ and $\ln z_B$.[11])

B. The mixing free energy

We assume the the distribution of A and B molecules in the aggregate (or any uniform, single-phase, portion thereof) is random. More specifically, it is assumed that the hydrophilic heads of A and B are randomly distributed over the (nearly) two-dimensional hydrocarbon–water interface. Because of electrostatic (or excluded volume) repulsions it is reasonable to assume that the head groups are organized in a lattice-like structure, executing only small fluctuations around their equilibrium positions, which occasionally lead to exchange of positions. According to this picture of ideal A,B mixing the A_M term in Eq. (1) is given by

$$A_M = -TS_M = kT[X_A \ln X_A + X_B \ln X_B]. \quad (15)$$

A few remarks should now be added:

(i) In liquid mixtures of molecules of different sizes, e.g., hydrocarbons of different chain lengths, the entropy of mixing is given by an expression analogous to Eq. (15) but with ϕ_K, the volume fractions, replacing X_K, the mole fractions. As in Flory–Huggins theory, this reflects proper counting of the possible configurations of two (or more) components with different molecular volumes.[32] Note, however, that our problem is different. The random mixing of the head groups is accounted for by Eq. (15), the configurational degeneracy associated with the various compatible organizations of the chains within the hydrophobic core already being taken care of by A_C.

(ii) If the actual sizes of the head groups are small compared to the average area per molecule at the interface, and the lateral diffusion of the amphiphiles is nearly free, the organization of the A,B heads is more appropriately represented as a ("semidilute") two-dimensional gas mixture. Then, a term accounting for the translational motion should be added to the right-hand side of Eq. (15). [This term is of the form $\sim \ln A$ where A is the interfacial area, or $\sim \ln(A/N)$ if a two-dimensional cell model is adopted.] The assumption that the head groups are nearly clamped at their equilibrium positions, as is appropriate to the small areas-per-molecule situations considered here, allows us to neglect this correction.

(iii) Clearly, Eq. (15) is most reasonable if the A and B head groups are similar. Otherwise, nonideal mixing becomes important, with corrections entering in lowest order via, say, a mean-field (Bragg-Williams)-type approximation.[32] This would require, however, some information on the nature of AA, BB, and AB interactions, and to keep the discussion general we ignore this complication.

C. The surface free energy

In the standard treatments of amphiphile aggregation and micellar growth the dependence of the aggregate free energy on its geometry is attributed solely to the surface term, A_S, in Eq. (1).[1,19] On the other hand, the hydrophobic cores of all aggregates are assumed to behave like bulk hydrocarbon droplets. Based on this picture one ignores the effects of geometry on chain conformational properties or, in other words, ignores the geometry dependence of A_C. One of our objectives here is to compare the relative influence of aggregation geometry on A_S and A_C for mixed (and as special cases, also for pure) aggregates. The surface interactions which determine A_S depend rather sensitively on the specific head groups involved. Yet, much insight has been gained into the role of the surface free energy from a general phenomenological picture of the "opposing forces." We shall adopt this simple but useful approach here for modeling A_S.

The opposing forces are: (i) The repulsion between head groups which tends to maximize the average area per molecule at the hydrocarbon–water interface, a. The leading term in the free energy associated with this effect is conveniently taken to be of the form C/a where C is a phenomenological constant[19] (which may be estimated independently in some cases). (ii) The hydrophobic effect or, more precisely, the surface tension between the hydrocarbon tails constituting the hydrophobic core and the aqueous solution, which tends to minimize hydrocarbon–water contact, hence a. This contribution to A_S is usually modeled as γa or $\gamma(a - \bar{a})$ where $\bar{a}$ is the bare head-group area; since $\gamma\bar{a}$ is just an additive constant it is irrelevant for calculating free energy *changes* and will, therefore, be ignored. γ is another phenomenological parameter, the micellar hydrocarbon–water surface tension. Combining the opposing forces one finds

$$A_S = \gamma a + C/a = 2\gamma a_0 + \gamma a(1 - a_0/a)^2, \quad (16)$$

where $a_0 = (C/\gamma)^{1/2}$ is the value of a which minimizes A_S. Note that if we assume, as in the standard treatments, that A_C is independent of geometry,[19] and thus also independent of a, the a_0 minimizes as well the *total* free energy $A = A_S + A_C$. Consequently, one often refers to a_0 as "the optimal area per head group."[19] However, we shall reserve this term for the value of a which minimizes A rather than only A_S.

Equation (16) applies to pure aggregates. If the head groups of A and B are identical or similar (e.g., both negatively charged), it may also be used for binary aggregates with $N = N_A + N_B$. In other cases, e.g., mixed aggregates of ionic surfactants and alcohol cosurfactants, Eq. (16) should be modified.[27] Here, however, we shall only consider binary aggregates for which Eq. (16) is appropriate.

A common hypothesis in the standard treatments of micellar structure stability is that the amphiphiles are always packed such that $a = a_0$, thereby minimizing their surface free energy. Simple geometric packing considerations reveal that in many cases the condition $a = a_0$ can be satisfied by more than one aggregation geometry. In such cases the preferred geometry is the one with highest surface curvature; because the corresponding aggregates are the smallest possible, hence, their number is maximal and so also the (translational or "mixing") entropy of the system. (For example, if both spherical and long cylindrical micelles satisfy $a = a_o$, spherical micelles will prevail.) Because the geometric packing criteria are nontrivially modified in the passage from pure to mixed aggregates, we examine them in some more detail.

D. Geometric packing constraints for mixed aggregates

Consider first pure aggregates. If, as assumed, the hydrophobic core is uniformly packed with chain segments, the "radius" R of the core cannot be larger than l, the length of

the fully extended (all-*trans*] hydrocarbon chain length: $R \leqslant l$. In a spherical or cylindrical micelle R is simply the radius, while in a bilayer it is its half-thickness. Let $\mathbf{v}$ denote the volume taken up by the hydrocarbon tail (as measured in the bulk liquid, say). Well-known volume–area relations then yield for our three "basic geometries":

$$a = k\frac{\mathbf{v}}{R} \geqslant k\frac{\mathbf{v}}{l} \equiv ka_t \tag{17}$$

with $k = 3$, 2, and 1 for spheres, cylinders, and planar bilayers, respectively. $a_t \equiv \mathbf{v}/l$ is the (average) cross-sectional area of an all-*trans* chain, which is also the minimal possible area per head group. (Of course $a = a_t$ is only possible in planar bilayers, for which $k = 1$.) Commonly used relations between $\mathbf{v}$ and l and the number of segments n in $-(CH_2)_{n-1}-CH_3$ chains have been proposed by Tanford.[1] These are $\mathbf{v} \simeq (n+1)v$ with $v \simeq 27$ Å^3 and $l \simeq n\delta$ with $\delta \simeq 1.27$ Å. Thus, according to this identification $a_t \simeq (v/\delta)(1 + 1/n)$ depends weakly on n.

Equation (17) sets simple but important lower limits on a for spheres $a \geqslant 3a_t$ and cylinders $a \geqslant 2a_t$. We shall now show that these lower limits can be significantly lower in mixed aggregates, depending on composition, a fact of relevance in calculating A_S via Eq. (16). Suppose $n_A > n_B$, i.e., the A chains are longer than the B chains. The volume of a hydrophobic core packed with N_A A chains and N_B B chains is $V = N_A\mathbf{v}_A + N_B\mathbf{v}_B$, and its surface area is $A = (N_A + N_B)a$ (recall, we assume similar head groups). It is easily verified that for spheres ($k = 3$), cylinders ($k = 2$), and bilayers ($k = 1$), $kV = AR$ where R is the "radius" of the aggregate as defined above. Clearly, $R \leqslant l_A$ where l_A is the length of the fully extended (longer) A chain. Thus, instead of Eq. (17) we now have

$$a = \frac{k}{R}(X_A\mathbf{v}_A + X_B\mathbf{v}_B) \geqslant \frac{k}{l_A}(X_A\mathbf{v}_A + X_B\mathbf{v}_B) \tag{18}$$

with $\mathbf{v}_A$ denoting the volume of an A chain, etc. Using for simplicity $\mathbf{v}_K = n_K v, l_K = n_K\delta, a_t = v/\delta \simeq \mathbf{v}_K/l_K = a_{t,K}$ [in actual calculations we use $\mathbf{v}_K(n_K + 1)v$], we can also write

$$\begin{aligned} a &= ka_t\frac{l_A}{R}\left(X_A + X_B\frac{n_B}{n_A}\right) \\ &= ka_t\frac{l_A}{R}\left[\frac{n_B}{n_A} + \left(1 - \frac{n_B}{n_A}\right)X_A\right]. \end{aligned} \tag{19}$$

This relation reveals that for a given R the average area per head group a decreases as the fraction of short chains B ($n_B < n_A$) increases. Conversely, for a given composition, a decreases as R increases. In particular, for $R = l_A$ we find that $a = ka_t(X_A + X_B n_B/n_A) \leqslant ka_t$ where the equality holds for $X_A = 1$ only, i.e., for pure A aggregates. Thus, for example, the last inequality implies that in mixed spherical micelles it is possible that $a < 3a_t$, as opposed to $a \geqslant 3a_t$ for single component micelles. Note, however, that the condition $a \leqslant ka_t$ by itself also implies the absurd conclusion that for bilayers ($k = 1$) it is possible that $a < a_t$. The source of this error lies not in Eq. (19), which holds for all k, R and X_A, but in the fact that for mixed aggregates $R \leqslant l_A$ is not the only constraint on R. More explicitly, in mixed aggregates the largest possible value of R depends also on composition (X_A) and geometry (k). To clarify this point, consider an aggregate with $l_B < R \leqslant l_A$. Clearly, the "inner region" of the core, of radius $R - l_B$, can only be reached by A chains (because B chains, even when fully extended, do not stretch that far). Thus, when $R > l_B$ the aggregate must contain enough A chains to fill up the inner region. This condition sets a lower limit on N_A for each $R > l_B$, or alternatively, an upper limit R for a given X_A. The restrictions on R (or X_A) are most stringent for bilayers, and least for spheres, as explained next.

Let f denote the fraction of A chain segments which can reach the inner region of the core: $f \simeq (n_A - n_B)/n_A = (\mathbf{v}_A - \mathbf{v}_B)/\mathbf{v}_A$. Then clearly we must require that

$$C_k(R - l_B)^k \leqslant N_A f\mathbf{v}_A \tag{20}$$

with $C_3 = 4\pi/3$, $C_2 = \pi L$ where L is the length of the cylindrical aggregate, and $C_1 = A$ where A is the surface area (of one face) of the bilayer. Also, since

$$C_k R^k = N_A\mathbf{v}_A + N_B\mathbf{v}_B \tag{21}$$

it follows that

$$\left(\frac{R - l_B}{R}\right)^k \leqslant f\frac{X_A\mathbf{v}_A}{X_A\mathbf{v}_A + X_B\mathbf{v}_B}. \tag{22}$$

This inequality sets a lower limit on X_A for any $R > l_B$, or an upper limit on R for a given X_A. (No restrictions apply to $R \leqslant l_B$.) If the limit on R implied by Eq. (22)—call it R^*—is larger than l_A, then of course $R \leqslant l_A$ is the relevant constraint. Otherwise, i.e., when $R \leqslant R^* < l_A$, the $R \leqslant l_A$ condition becomes superceded by the requirement that the inner core be filled with A. After determining the allowed regimes R and X_A the average area per head group can be calculated from Eq. (19). From Eq. (22) we see that for larger k, i.e., higher curvature, lower values of X_A are allowed, hence according to Eq. (19) lower values of a/ka_t. Note in particular that for bilayers, $k = 1$, $R = l_A$ is only possible for $X_A = 1$ [because $f \simeq (l_A - l_B)/l_A$], whereas for $X_A < 1$ the bilayers' half-thickness R is necessarily smaller than l_A. The combination of Eqs. (22) and (19) reveals that for $k = 1$, $a \geqslant a_t$ for all compositions, as expected. On the other hand, for spherical micelles $k = 3$, the lowest limit on X_A for $R = l_A$ is significantly lower than 1, indicating via Eq. (22) that a may be significantly smaller than the $3a_t$ limit for pure spherical micelles. The main consequence of this result is that *mixed curve aggregates can be packed with relatively low areas per head group*. Thus if, say, a_0 in Eq. (16) is smaller than $3a_t$, then pure aggregates are relatively unstable as spherical micelles, whereas this need no longer hold in the mixed case.

In Fig. 2 we show the minimal area per head-group a (or maximal radius R) for mixed spherical and cylindrical micelles, as a function of composition. The calculation was done here for a mixture of $-(CH_2)_{10}-CH_3$ ($=A$) and $-(CH_2)_4-CH_3$ ($=B$) chains, using $l_K = n_K\delta$ and $\mathbf{v}_K = (n_K + 1)v$ with $v = 27$ Å^3, $\delta = 1.27$ Å. The area per head group is expressed in units of $a_t = 22$ Å^2. (This value of a_t is slightly higher than $v/\delta = 21.2$ Å^2 because $a_{t,K} = \mathbf{v}_k/l_k \simeq v/\delta$. Clearly the choice of a_t does not affect any of our conclusions.) The minimal values of a in the two limits $X_A = 1$ and $X_B = 1$ are not exactly the same, cf.

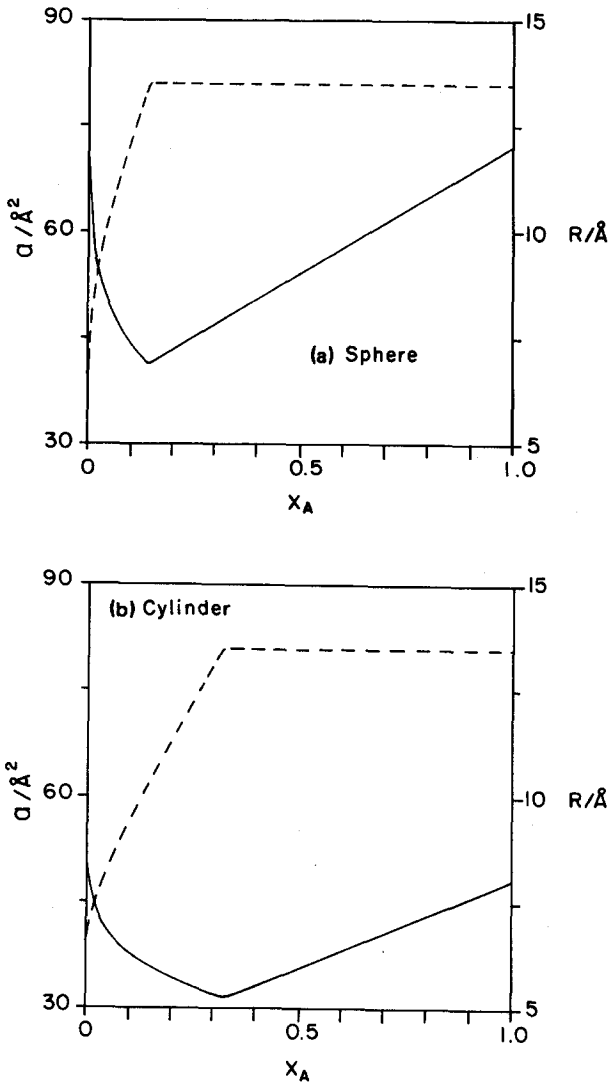

FIG. 2. Minimal area per head group a (solid line, left scale) and maximal radius R (dashed line, right scale) in mixed spherical (a) and cylindrical (b) micelles composed of 11-carbon and 5-carbon chains, as a function of the fraction of long chains (X_A), calculated from Eqs. (19) and (22). Note the substantial decrease of the minimal a at intermediate compositions, compared to those of the pure aggregate; see the text.

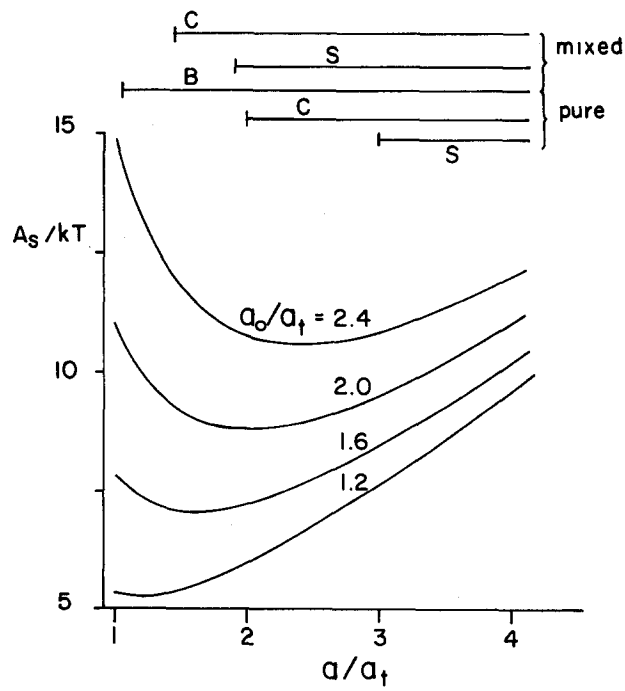

FIG. 3. The surface free energy as a function of the area per head group, calculated from Eq. (16) with $\gamma = 0.1kT/\text{Å}^2$, for $a_0/a_t = 1.2, 1.6, 2.0$, and 2.4. ($a_t \simeq 22$ Å^2 is the cross sectional area of an all-*trans* chain.) The horizontal lines at the top of the figure indicate the regimes of allowed a values for pure and mixed planar bilayers (B), cylinders (C), and sphere (S).

Eq. (17), because v_K/l_K depends weakly on $K(=A,B)$. Note the significant decrease in (the minimally allowed) a for intermediate X_A values e.g., for $X_A = 0.2$ $a \simeq 2a_t$ compared to $a \geqslant 3a_t$ for the pure case. Similar effects, though less pronounced, characterize cylindrical micelles.

In Fig. 3 we show the surface free energy A_S as a function of the average area per head group (in units of a_t), calculated from Eq. (16) for several values of a_0. ($a_0/a_t = 1.2, 1.6, 2.0$, and 2.4.) The value of γ used in these calculations, $\gamma = 0.1kT/\text{Å}^2$ (corresponding to $\simeq 40$ dyn/cm at 300 K) is of the order of the oil/water interfacial tension (~ 50 dyn/cm). The figure also contrasts the regimes (lower limits) of a values allowed for different aggregation geometries for pure and mixed aggregates, as determined by Eq. (17) and by Eqs. (18) and (22), respectively. It is seen clearly that the overlap between the regimes of allowed a values for different geometries is substantially larger for mixed aggregates. Note in particular that as a_0 increases (i.e., already for $a_0 \geqslant 2a_t$) all geometries are allowed with $a \simeq a_0$.

III. RESULTS AND DISCUSSION

In this section we present a series of calculations of chain conformational properties and thermodynamic functions for mixed spherical, cylindrical, and planar bilayer aggregates. All calculations are for mixtures of eleven-carbon h_A–$(CH_2)_{10}$–CH_3 ($n_A = 11$), and five-carbon h_B–$(CH_2)_4$–CH_3 ($n_B = 5$) amphiphiles. The headgroups h_A,h_B are assumed identical. The chains are modeled using the rotational-isomeric-state model,[31] with $e_g = 500$ K and $T = 300$ K. The parameters α_i (lateral pressures π_i) are evaluated by solving the constraint equations (5) [using Eqs. (12) and (13)] for the appropriate composition X_A and geometry $\{\rho_i m_i\}$. For each geometric boundary condition, i.e., an interface of a given curvature, all the allowed bond sequences of A and B molecules are generated by matrix multiplication. For each bond sequence we randomly sample 3 head-group positions within a range Δz (typically $\Delta z \simeq 1.4$ Å) perpendicular to the interface, and 12 head orientations (i.e., 36 configurations) and keep only those for which no chain segment protudes beyond the micellar interface. Further details are given elsewhere.[12]

In a previous paper we studied the role of surface roughness fluctuations by allowing the segment density near the interface to be lower than its bulk liquid value.[12] More spe-

cifically, the hydrophobic core was divided into L layers of width $\sim$1–2 Å. ($L\sim$5–7 and 10–14 for curved and planar aggregates, respectively.) Surface roughness, over a range of about $\sim$2–4 Å has been introduced by choosing $\rho_1 \leqslant \rho_2 \leqslant \rho_3 \leqslant = \rho_4 \cdots = \rho_L = 1$ and it was concluded that bilayers are appropriately described by an essentially sharp interface, i.e., $\rho_1 = \rho_2 = \cdots = \rho_L$. On the other hand, for spherical micelles comparison between theory and experiment suggests a higher (though limited) extent of surface roughness, e.g., we found that a density profile with $\rho_1 = 0.35$, $\rho_2 = 0.70$, $\rho_3 = \cdots = \rho_L = 1$ provides good agreement with available data. Recent molecular dynamics simulations support this conclusion.[17,18] We have thus used this density profile in all the calculations for spherical micelles presented below. It should be noted however that results are not very sensitive to small variations in ρ_i; even "compact " spherical micelles ($\rho_1 = \rho_2 = \cdots = \rho_L = 1$) show similar *qualitative* behavior. For cylindrical micelles an intermediate interface profile is appropriate: we have taken $\rho_1 = 0.12, \rho_2 = 0.90, \rho_3 = \cdots = \rho_L = 1$.

The results will be presented in two parts. The first describes the *conformational statistics* of the long (A) and short (B) chains, and their dependence on micellar composition and geometry. The second part deals with the *thermodynamic* implications of geometry, composition, and surface vs core contributions to the free energy of the aggregate.

A. Conformational properties

Replacing part of the long chains (A) in a pure A aggregate by short chains (B), or vice versa, modifies the conformational statistics of the remaining molecules. The changes attendant upon chain mixing depend on composition and aggregation geometry and are reflected by various properties. One of those is the spatial distribution of chain segments as a function of the distance from the aggregate's interface. Figure 4 illustrates how the volume of a bilayer is filled up by A and B chain segments. The figure shows the fraction of the ith layer which is filled by K-chain segments: $X_K \langle \phi_{i,K} \rangle / m_i$ ($K = A,B$ and in this case m_i = constant and $\rho_i = 1$, i.e., sharp interface). For clarity of presentation we have transformed here from the (discrete) layer index i to z—the distance from one interface. Figures 4(a) and 4(b) correspond to two different compositions, $X_A = 2/3$ and 1/3, respectively, but the average area per molecule is the same, $a = 27$ Å^2. In both cases the bilayer's half-thickness is larger than l_B, the length of a (fully extended) B chain, and smaller than l_A. Thus, the central region of the bilayer can only be filled by A-chain segments, while the short-chain segments occupy regions closer to the two interfaces (as pictorially depicted in Fig. 1). This behavior is reflected by the shift in the maximum of $\langle \phi_{i,A} \rangle$ towards the bilayer's midplane as X_A decreases from 2/3 to 1/3. For comparison, in pure A bilayer with this area per head group, $\langle \phi_{i,A} \rangle$ is constant, except near the bilayer's midplane, where it drops rapidly to zero as the chains cross the midplane (chain "interdigitation"). Figure 4(b) demonstrates clearly both the crowding of A chain segments near the midplane and the large extent of interdigitation.

Figure 5 shows $X_K \langle \phi_{i,K} \rangle / m_i$ for two spherical micelles

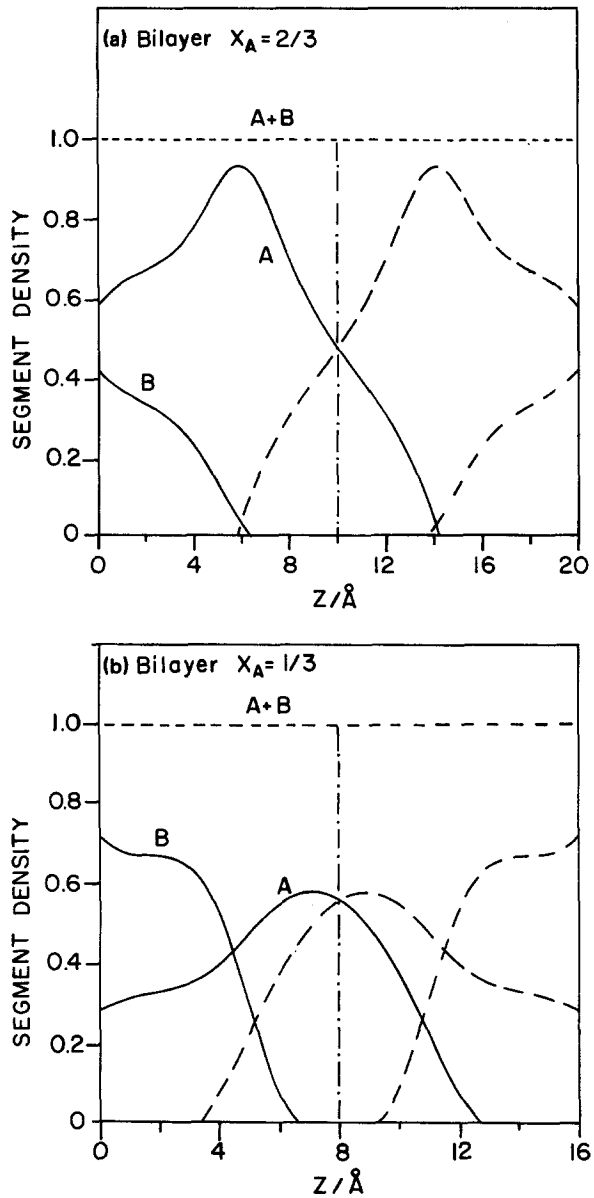

FIG. 4. Density profiles of long-chain segments (A) and short-chain segments (B) across a mixed planar bilayer. (a) $X_A = 2/3$, (b) $X_A = 1/3$. In both figures the average area per chain is $a = 27$ Å^2. Correspondingly, the total widths of the bilayer are different; 20 Å for $X_A = 2/3$ and 16 Å for $X_A = 1/3$. z is the distance from the "left" bilayer's interface, and is proportional to the layer index i. [The continuous curves are obtained by connecting the data points for the layers i using $z = (i - 1/2)d$ where d is the layers' width, cf. Fig. 1.] Specifically, the curves marked A and B show $X_K \langle \phi_{i,K} \rangle / m_i$ [or equivalently $X_K \langle \phi_K(z) \rangle / m(z)$], $K = A,B$. The solid curves correspond to chains originating from the "left" ($z = 0$) interface, while the dashed curves are for those originating from the "right" interface. Note that the sum of all chain-segment densities corresponding to a given z adds up to the total segment density, here normalized to 1 and designated by the dashed line marked "A + B". The vertical (dash–dotted) line indicates the midplane of the bilayer. The figures clearly demonstrate the confinement of the short chains to the outer regions of the bilayer, and the stretching of the long ones to the inner volume, which is particularly pronounced at small values of X_A (and small areas per head group).

of the same radius but with different amphiphile compositions (i is replaced by r). In Fig. 5(a), $X_A = 0.8$, i.e., we have nearly pure A micelle (volume fraction of $A \sim 0.9$); here the presence of small amounts of B chains is just a small perturbation. But again, as in bilayers, when most of the chains are

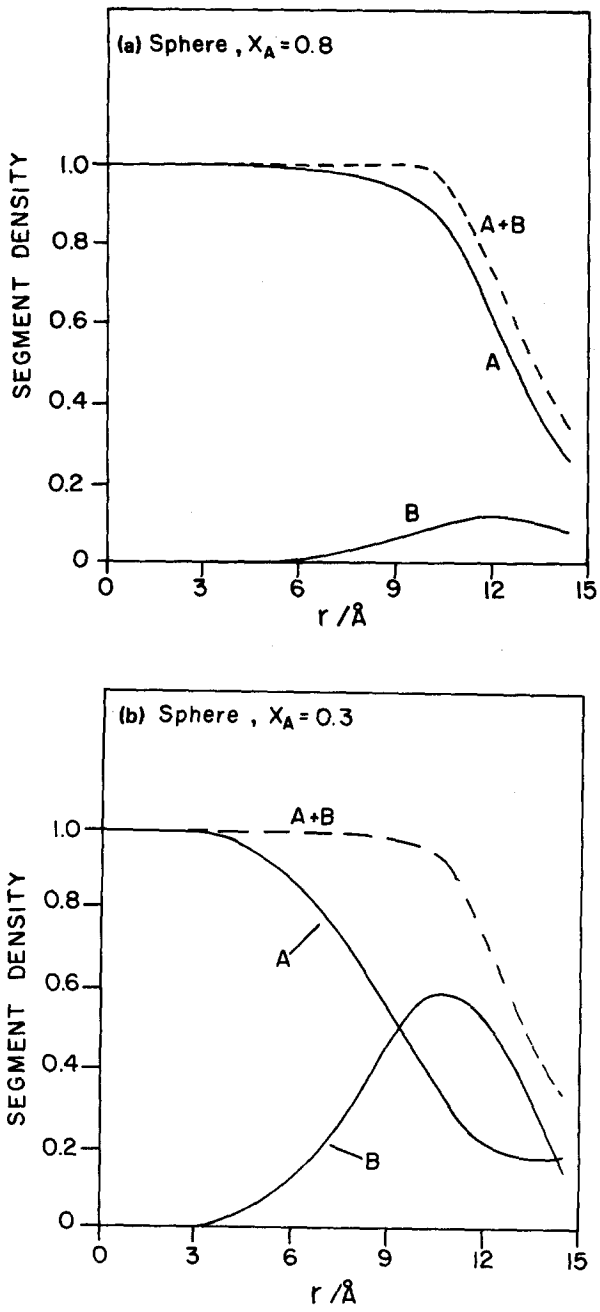

FIG. 5. Segment density profiles in mixed spherical micelles. (a) $X_A = 0.8$, average area per head group $a = 77$ Å^2, average micellar radius (average head group distance from center) $R = 13.4$ Å. (b) $X_A = 0.3$, $a = 53$ Å^2, $R = 13$ Å. r is the distance from the center of the micelle. [The curves are constructed by connecting the data points for the imaginary layers i, using $r = (R - i + 1/2)d$ where d is the layers' width, cf. Fig. 1.] The curves marked by A, B, and A + B have the same meaning as in Fig. 4. Note however that in the present case the total segment density profile (A + B) decreases towards the surface of the micelle corresponding to "surface roughness" (Ref. 12). The stretching of the long chains (in order to fill the inner volume of the micelle) is mainly apparent for small X_A values [Fig. 5(b)].

short, the long ones are pushed into the center of the aggregate: see Fig. 5(b), where $X_A = 0.3$. Similar behavior is observed for cylindrical micelles. (Cylinders always reveal an intermediate behavior between the spherical and planar aggregates and, therefore, will not be discussed further in this section.)

The presence of short chains B in an aggregate of radius $l_B < R < l_A$ imposes stretching of the "first" part (of length comparable to l_B) of the longer chains A and subsequent "squashing" of the "second" part of these chains (of length $\sim l_A - l_B$) which must fill up the inner volume of the aggregate. This is consistent with (rather qualitative) analyses based on ^{13}C NMR measurements.[21,22] Conformational changes associated with chain mixing should be reflected not only in the $\langle \phi_{i,K} \rangle$s, but also in more detailed conformational properties, such as bond parameter profiles and segment radial distributions. Both are measureable properties but, unfortunately, no systematic studies have been reported so far for mixed aggregates. Partial information is available for only a few specific systems, as mentioned below.

The orientational ("P_2") order parameter of a C–C or C–H(C–D) bond, is defined as

$$S = \langle P_2(\cos\theta) \rangle = 3\langle \cos^2\theta \rangle/2 - 1/2,$$

where θ is the angle between the bond and the normal to the micellar interface (the "director"). If the bond in question is perfectly parallel to the director $S = 1$, whereas if the bond is perpendicular $S = -1/2$. For a random distribution of bond-director angles $S = 0$. As a reference for comparison, $S = -1/2$ for all C–D bonds for an all-*trans* chain oriented normal to the interface. Thus, in Fig. 6 (and other C–H bond order profiles) we show $-2S_{C\text{-}D}$ whose maximal value is 1. (We denote the bonds as C–D rather than C–H because experimentally S is usually measured by the quadrupolar NMR splitting of selectively deuterated C–H bonds.[6,14])

Figure 6 shows the (C–D) bond order parameters of A and B chains packed in bilayers at different compositions, with a similar average area per head group for all cases ($a \simeq 33$ Å^2). The bond order profiles reveal that the first few bonds of the longer chains are rather insensitive to the presence of the short ones [cf. Fig. 6(a)]. The distortion due to the short chains is apparent in the farther portions of the chains which are "squashed" in order to fill up the central region of the bilayer. This requires substantial chain bending and consequently a decrease in the order parameters, which becomes more stringent at high X_B values. This behavior of the beginning and end of the long chains, upon "dilution" by shorter ones, is observed by Mely and Charvolin[20] in their NMR order parameter studies of C_{18}/C_{10} soap mixtures in lamellar bilayers (see, say, their Fig. 3). Stretching the long chains involves a higher free energy price than that associated with stretching the short ones. By stretching themselves a little the short chains can significantly reduce the free energy burden on their long neighbors, giving rise to an increase in S for the short chains as X_A decreases [cf. Fig. 6(b)]. This stretching of the short chains is consistent with the analysis in Ref. 22.

Figure 7 shows the order parameters of the long chains when packed, at different compositions, in a spherical micelle of constant radius ($R \sim 13$ Å). Since R is constant, an increase in X_B corresponds to replacing long chains by (about twice as many) short ones. This implies a decrease in the average area per head group and consequent "squeezing" of both the A and B chains reflected by increasing values of the order parameters.

Another common characteristic of chain packing in micellar aggregates is the spatial distribution of the various chain segments, particularly of the terminal (CH_3) groups.

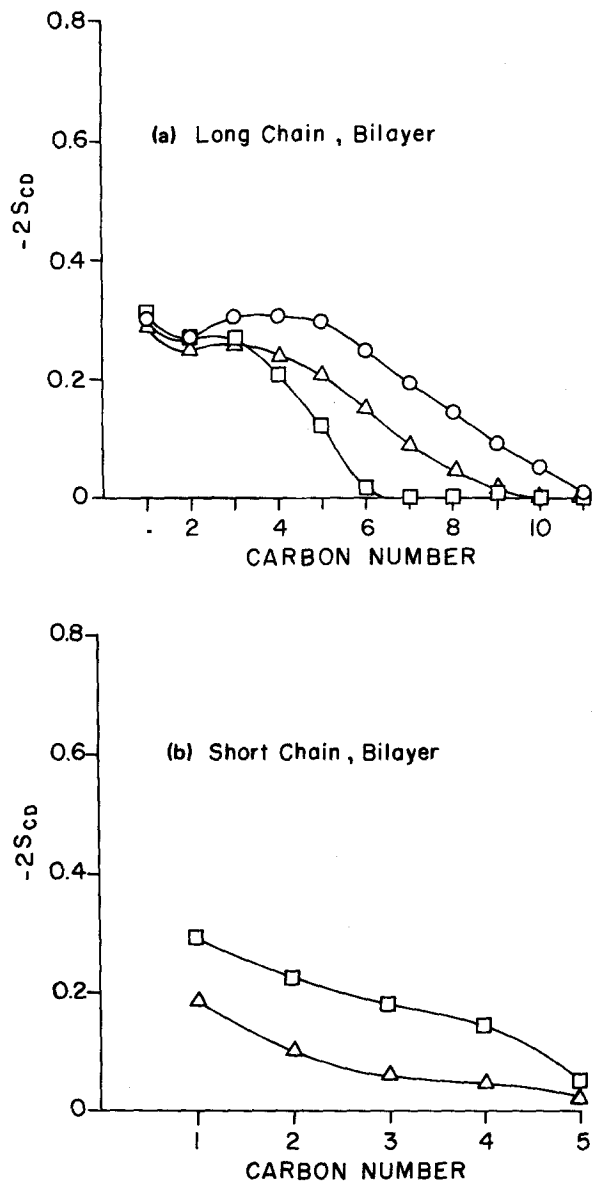

FIG. 6. Bond order parameter profiles ($-2S_{CD}$) of: (a) the long (11-carbon) chains, and (b) the short (5-carbon) chains packed together in mixed planar bilayers. Different curves correspond to different compositions but in all cases the average area per head group is (nearly) the same. ○: $X_A = 1.0, a = 32.4$ Å^2, △: $X_A = 2/3, a = 33.75$ Å^2, □: $X_A = 0.2, a = 32.4$ Å^2.

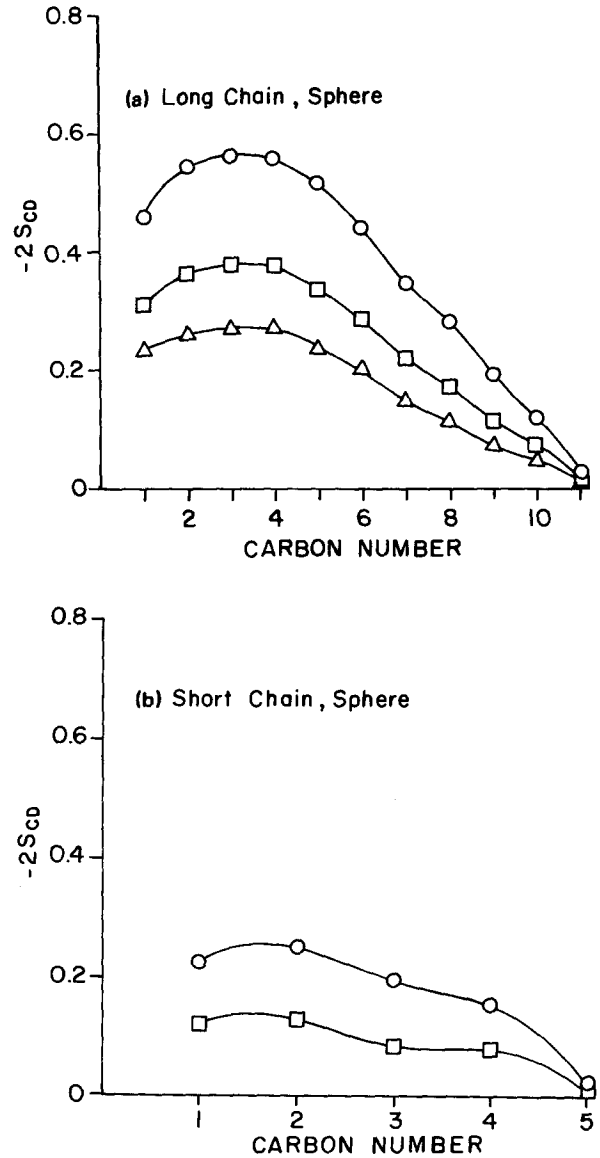

FIG. 7. Bond order parameter profiles of: (a) the long (11-carbon) chains, and (b) the short (5-carbon) chains packed together in mixed spherical micelles. In all cases the average micellar radius is the same $R \cong 13.2$ Å. △: $X_A = 1.0$, □: $X_A = 0.5$, ○: $X_A = 0.2$.

Figure 8 shows the (unnormalized) probability of finding the terminal group of the long chain at a distance z from the bilayer's interface, for three different compositions but the same area per head group ($a \simeq 33$ Å^2). In one-component bilayers the distribution of chain termini peaks around the midplane. As the fraction of short chains ($X_B = 1 - X_A$) increases the peak of the distribution crosses the midplane, indicating enhanced interdigitation of chains anchored to opposite interfaces. This reflects the increasing statistical weight of those long-chain conformations which reach the "other half" of the bilayer compared to those which are confined to the half from which they originate. Note, however, that the shift is not very pronounced. The shift in the termini distribution is expected to be even less marked for curved aggregates (with variable X_A and fixed a), because of the smaller "inner volume" (which cannot be reached by the short chains) around the center of the aggregate. Indeed, our calculations for spherical micelles with constant a and varying X_A confirm this notion. (Note that to span the entire range of X_A values a must be at least $3a_t$ which is the minimal area per head group for both $X_A = 0$ and 1.)

On the other hand, if spherical micelles of different compositions could be prepared with the same *radius* then, the terminal group distribution would show strong dependence on X_A, as shown in Fig. 9. Explicitly, when X_A is large most long chains terminate in the outer regions (near the surface) of the micelle, simply because the central regions are small and do not allow chain crowding.[11-13,27] As X_A decreases, i.e., long chains are replaced by shorter ones (and R is kept constant), it can only be at the expense of those long chains

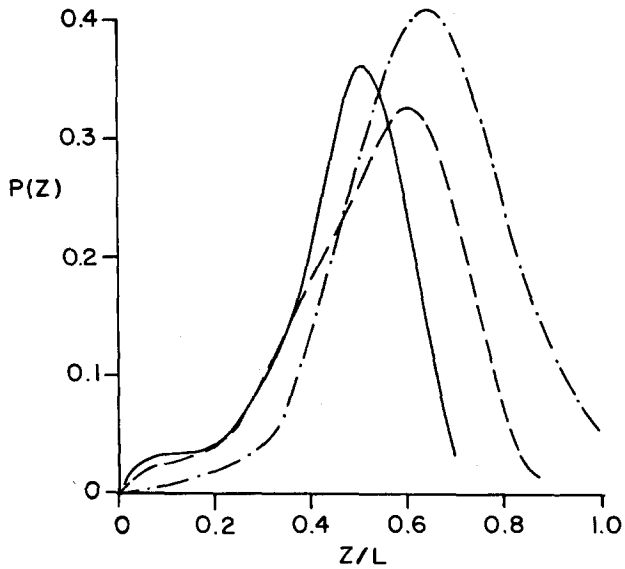

FIG. 8. The (unnormalized) probability of finding the terminal (CH_3) segment of the long chain at distance z from one interface of a mixed planar bilayer. (Here L is the width of the bilayer.) Different curves correspond to different compositions but the average area per head group is nearly constant. The full line corresponds to $X_A = 1.0$, $a = 32.4$ Å^2, the dash–dotted line to $X_A = 0.2$, $a = 32.4$ Å^2 and the dashed line to $X_A = 2/3$, $a = 33.75$ Å^2.

which do not reach the central region of the micelle (simply because the short chains do not stretch so far). This of course increases the fraction of "stretched" long chains and consequently shifts the termini distribution towards the center of the micelle. Note, however, that keeping R constant implies a change in the average area per head group, cf. Eq. (19). For a mixture of short and long chain surfactants with the same (e.g., ionic) head group the optimal a is largely determined by the surface ("opposing") forces (i.e., $a \sim a_0$) and, hence, preparing mixed micelles of these molecules with the same radius is probably impractical. On the other hand this may be relevant for mixed micelles comprised of, say, long ionic surfactants and short chain nonionic amphiphiles (e.g., alcohols).

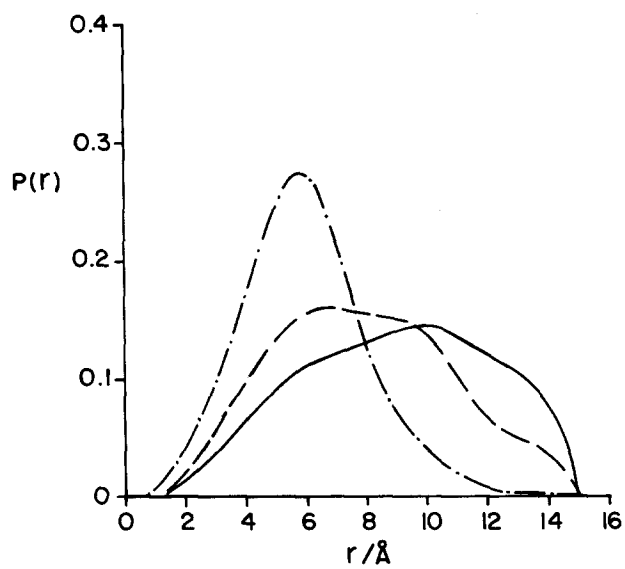

FIG. 9. The (unnormalized) probability of finding the terminal (CH_3) segment of the long chain at distance r from the center of a mixed spherical micelle, for different compositions. Full line $X_A = 1.0$, dashed line $X_A = 0.5$ and dash–dotted line $X_A = 0.2$. In all cases the micellar radius is $R \cong 13.2$ Å.

B. Free energies

As noted in Sec. II C, in the standard models of micellar stability the preferred micellar geometry is determined only by the surface free energy A_S.[1,19] Specifically, A_S is assumed to depend only on the average area per head group a leading, e.g., to the "opposing forces" representation, Eq. (16) and Fig. 3. Furthermore, the chain contribution to the free energy is assumed independent of a and the curvature of the aggregate.[19] It has already been noted (for pure aggregate) that there is no obvious justification for this assumption.[11–13] Figure 10 supports this reservation for both pure and mixed aggregates. The figure shows A_C the conformational free energy per chain [see Eqs. (9)–(14)], as a function of the average area per head group for the three micellar geometries considered in this paper. The curves corresponding to $X_A = 1/2$ include the contribution of the mixing entropy A_M, cf. Eq. (15). Note that this only adds a constant term to A_C, for all geometries.

Comparing Fig. 10 with Fig. 3 we note that the variations of A_C with a are comparable to those of A_S. Focusing for a moment on the A_C curves for *pure* aggregates ($X_A = 1$) we see that the minima in A_C occur at different $a \equiv a^*$ values for the different aggregation geometries; a^* increases from bilayers to cylinders to spheres. Also, A_C increases sharply as a falls significantly below a^*. The increase in A_C for $a > a^*$

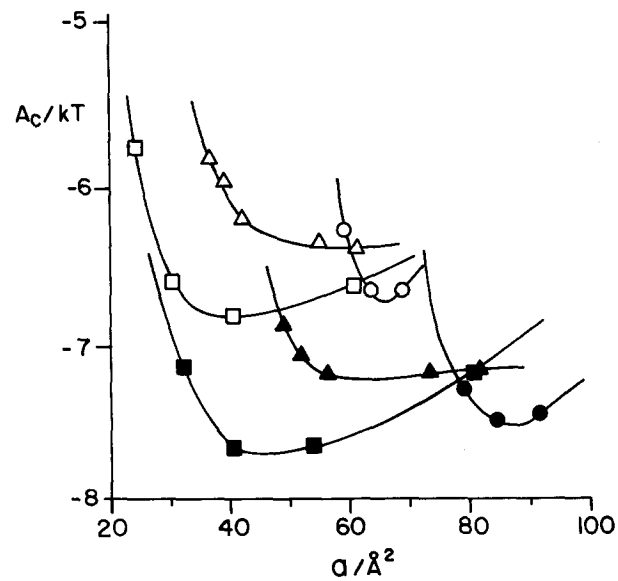

FIG. 10. The conformational free energy A_C as a function of the average area per head group for the three basic geometries: planar bilayers (squares), cylindrical micelles (triangles), and spherical micelles (circles). The solid symbols are for pure aggregates of long chains ($X_A = 1.0$). The open symbols are for "equimolar" ($X_A = X_B = 1/2$) aggregates of 11-carbon and 5-carbon chains. In the latter case the curves show the sum $A_C + A_M$ (note however that A_M is constant). The zero of the free energy scale corresponds to an all-*trans* chain.

is more moderate. For planar bilayers this behavior is easily understood; small a values correspond to significant chain stretching which involves a high free energy price. For $a > a^*$ the chain is "squashed", hence, distorted, yet even as a goes to its maximal value, i.e., a very thin bilayer, the chains are essentially two dimensional and thus have a nonzero conformational entropy. This explains the relatively moderate increase in A_C for $a > a^*$. The sharp rise of A_C for $a < a^*$ for spheres and cylinders, is simply due to the existence of a finite lower limit on a for chain packing at uniform density for these geometries [cf. Eq. (17)]. In this context it is interesting to recall the basic premise of the picture in which only surface (opposing forces) effects are considered. The quantitative implication of such models would be to approximate all the A_C curves (for both $X_A = 1$ and $X_A \neq 1$) by "L-shaped" curves such that A_C is infinite for $a < a^*$ and constant for $a > a^*$, and moreover that A_C ($a \geqslant a^*$) is the same for all geometries. This is obviously a drastic approximation and the question is how good is it for determining the relative stability of different aggregation geometries. We shall consider this point in some more detail shortly.

Some similar qualitative trends in the behavior of A_C are revealed in Fig. 10 for the mixed aggregates. The important effect of chain mixing is the shift in the a^*, i.e., the value of a where A_C is minimal, towards lower values. Thus, in mixed aggregates not only the range of allowed head-group areas extends (for the curved geometries, see Fig. 3) to lower a values, but a^* is lower as well. Note however that a_0, the optimal area per head group dictated by A_S only, is independent of composition, cf. Eq. (16) (for amphiphiles with similar head groups).

Returning to Eq. (1) we note that A_S attains a minimum at $a = a_0$ (which depends on the nature of the head groups but is independent of chain length, geometry, or composition), whereas A_C is minimal at $a = a^*$ which depends on geometry, composition, and of course chain lengths as well. For a given composition A_M is constant: Hence, the minimum in $A = A_C + A_M + A_S$ will occur at some value a_m which, in general, is different from both a_0 and a^* and which varies with micellar geometry. When considering different composition, X_A the contribution of A_M should also be added; clearly this term is maximal for $X_A = X_B = 1/2$ (and vanishes identically for $X_A = 0$ or $X_B = 0$). We now turn to a more quantitative examination of these notions and their implications with respect to micellar stability. Of particular interest is the question of whether the "hierarchy" of stability of the various geometries may vary with composition.

The shape (spherical, planar, etc.) of an aggregate and its composition do not suffice to specify its dimensions, e.g., spherical micelles with given X_A can have different radii, hence different areas per head group (and, correspondingly, different $N = N_A + N_B$), see Eq. (18). There is of course a specific value of the area per head group a^* (or radius R^*) for which A_C of a micelle with a given shape obtains a minimum, as was shown in Fig. 10 for two specific compositions. Figure 11 displays these minima as a function of composition, X_A, for the three geometries studied. More precisely, the figure shows $A_C(a = a^*, X_A) + A_M(X_A)$ vs X_A. Note that A_M is independent of geometry, hence, the addition of this term does not alter the stability hierarchy of the different aggregation geometries for any of the compositions.

Figure 11 reveals that as far as chain packing is concerned the relative stabilities of the different geometries are independent of composition. In particular chain packing in planar aggregates is most favorable for all compositions. It should be noted that the higher stability of spherical micelles compared to cylindrical ones, is a result of the different roughness (ρ_i) profiles assumed for these geometries. For aggregates with (equally) sharp interfaces (same ρ_i), cylindrical micelles are more stable. As noted earlier, and in detail elsewhere, the detailed nature of surface roughness is a matter of controversy[12,13,28,29] and our choice of density profiles has been guided by somewhat indirect experimental and theoretical evidence.[12] Yet, this question is irrelevant for the following discussion.

After analyzing the minima in the separate contributions A_S and $A_C + A_M$ to the aggregate's free energy, we now turn to the sum $A = A_C + A_M + A_S$. As noted above, the minimum in A for given composition X_A, and geometry (spherical, planar, etc.) will occur at some $a = a_m$ which differs from both a_0 and a^*. Of course a_m depends not only on X_A and the aggregation geometry but also on a_0 [or, in other words, on the strength of the surface forces in Eq. (16)].

Figures 12(a)–12(c) display the minimal values of the total free energy $A(a = a_m)$ as a function of composition for different values of a_0; $a_0/a_t = 1.2$, 1.8, and 2.4. Consider first Fig. 12(a), for which $a_0 = 1.2a_t \simeq 26$ Å^2. Clearly, only planar bilayers can be packed such that the average area per molecule $a \sim a_0$. The minimal value of a for pure spherical micelles ($X_A = 1$ or 0) is $a \sim 3a_t$ and even for mixed micelles $a \geqslant 45$ Å$^2 \simeq 2a_t$ [see Fig. 2(a)]. Similarly, cylindrical mi-

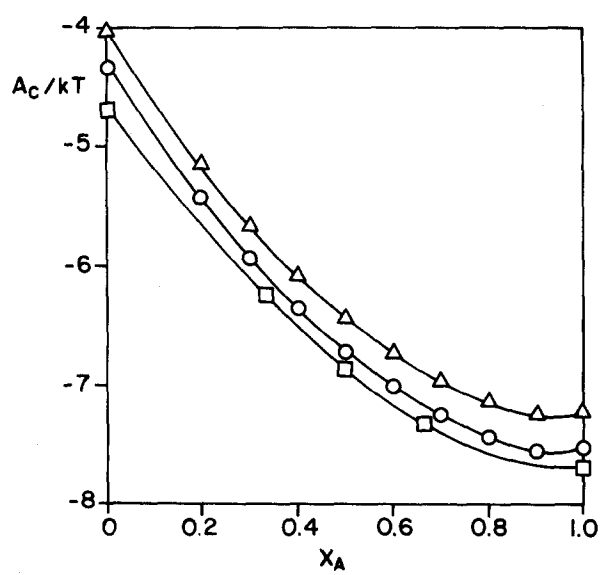

FIG. 11. The sum of conformational and mixing free energies per molecule $A_C + A_M$ for optimally packed mixed aggregates of 11-carbon (A) and 5-carbon (B) chains as a function of composition: squares: planar bilayers, triangles: cylindrical micelles, circles: spherical micelles.

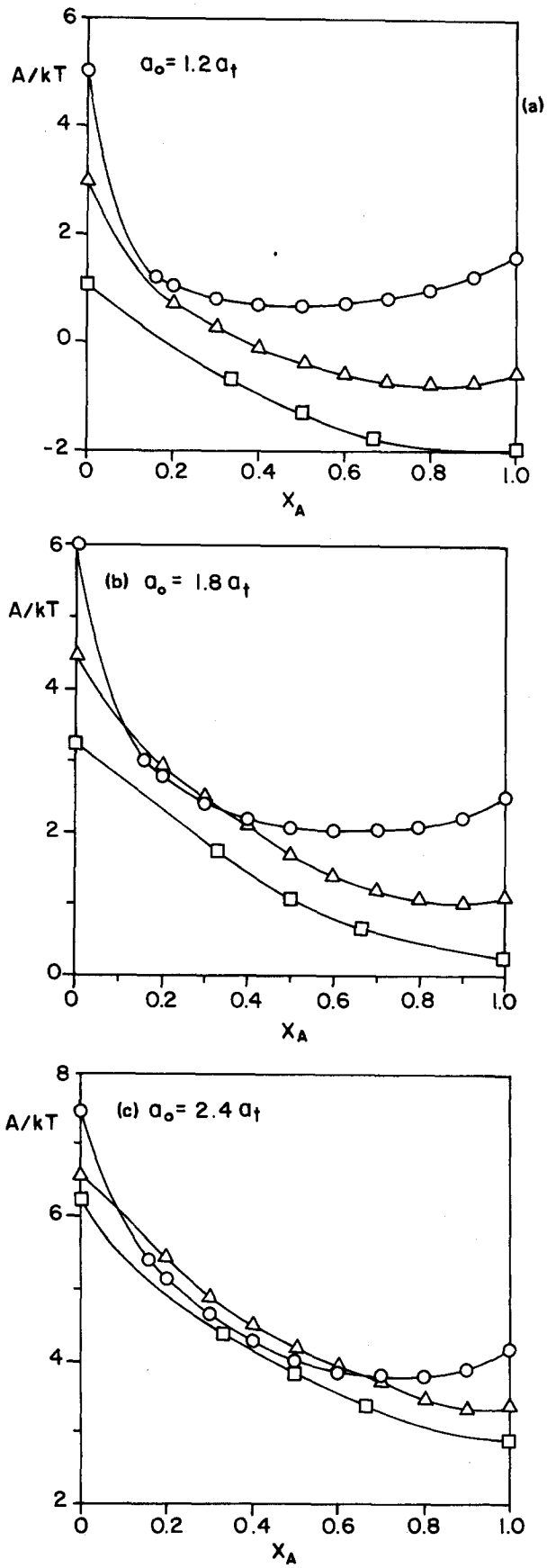

FIG. 12. Minimal values of the total free energy per molecule $A = A_C + A_M + A_S$, for mixed aggregates of 11-carbon (A) and 5-carbon (B) chains, as function of composition X_A. The surface free energy depends on a_0 and γ, cf. Eq. (16). In all cases $\gamma = 0.1kT/\text{Å}^2$. The values of a_0 used are $a_0/a_t = 1.2$ (a), 1.8 (b), and 2.4 (c) ($a_t = 22$ Å^2).

celles can only exist with $a \geqslant 1.4a_t$. Hence, according to Eq. (16) (see also Fig. 3) the surface free energy A_S is very high for all the allowed a values of the two curved geometries, particularly so for the spheres. The difference $A_S(\text{sph}) - A_S(\text{cyl}) > 0$ is large enough to offset $A_C(\text{sph}) - A_C(\text{cyl})$ (Fig. 11), and thus raise the sphere free energy above that of the cylinder for all X_A. Note also that $A_C(\text{sph}) - A_C(\text{cyl})$ is nearly constant for all X_A. Thus, the approach of the $A_C(\text{sph})$ curve to that of $A_C(\text{cyl})$ near $X_A \sim 0.2$, is mainly due to the fact that for this X_A there is a significant decrease in the minimally allowed a_{sph}, cf. Fig. 2(a). We may thus conclude that for low values of a_0 (e.g., $1.2a_t$) the free energy is almost exclusively dominated by geometric packing constraints and their manifestation in the surface free energy [Eq. (16)].

As a_0 increases and "approaches" the regime of a values allowed for the curved geometries, the simple geometric packing constraints which determine the range of possible a's become less stringent. Consequently, we expect still smaller differences in A_S between the various geometries and an increasingly important role for the conformational free energy. Indeed, this trend is clearly exhibited in Figs. 12(b) and 12(c). From Fig. 12(b) we see that for $X_A \sim 0.2$, spherical and cylindrical micelles are nearly equally stable. (Thus, in isotropic solutions one might expect mixed spherical micelles to prevail, due to their higher "mixing" entropy, i.e., more particles.) The X_A dependence of the differences in A corresponding to different geometries suggests that the stability hierarchy may vary with composition.

Figure 12(c) displays A vs X_A for $a_0 = 2.4a_t \simeq 53$ Å^2. For pure aggregates such areas per head group are typical for cylindrical micelles, while spherical micelles are excluded because they require $a > 3a_t$. This is no longer the case for mixed systems where, for $X_A \sim 0.1$–0.4, spheres are allowed with $a \sim a_0$ (and of course cylinders and bilayers). In this range of compositions, then, the relative stability of different aggregation geometries will be dominated by the conformational free energy. As Fig. 12(c) reveals, for $X_A \sim 0.1$–0.5, spherical micelles are (a little) more stable than cylindrical ones, and are nearly as stable as planar bilayers. Translational ("mixing") entropy will further favor the smaller aggregates.

Charvolin and Mely have studied the phase behavior of $C_{18}K/C_NK$, $N = 10,14$ (potassium soaps) mixtures, as a function of composition.[24] They found that the $C_{18}K/C_{14}K$ mixtures form stable bilayers at all compositions. On the other hand, in mixtures of the more dissimilar $C_{18}K/C_{10}K$ molecules, stable lamellar phases of bilayers are formed when the mole fraction of the longer chains X_A is either small ($X_A \leqslant 0.2$) or large ($X_A \geqslant 0.8$). At intermediate compositions however, a new phase appears. Thse experiments suggest that this phase is cubic, and the amphiphiles are packed with an area per head group of ~ 47 Å^2, consistent with micellar interfaces of higher curvature. The areas per head group in the lamellar phases are ~ 37 Å^2 for both $X_A \sim 0$ and $X_A \sim 1$. While no direct quantitative comparison with our calculations can be conclusive at this point, it is interesting to note, as shown in Figs. 12(b) and 12(c), that indeed the curved aggregates are nearly as stable as the bi-

layer at intermediate X_A, but not at the two extremes $X_A \sim 0$ or 1. Note in particular that in Figs. 12(b) $a_0 = 1.8a_t \sim 39$ Å^2. For bilayers $a_m \simeq a_0 \simeq 39$ Å^2 is close to the area per head group observed experimentally.[24] Furthermore, the areas per head group corresponding to the minimal free energies of the spherical micelles at $X_A \sim 0.3$ are $a_m \sim 50$ Å^2. Of course this comparison should not be driven beyond its qualitative aspects, since the chains that we have modeled are about half as long as those studied experimentally. Yet it should also be noted that for doubly long chains, all the conformational free energies are (roughly) doubled as well, a fact which may possibly lead to interesting "free energy curve crossing." Finally, it is clear that all the effects due to packing of dissimilar chains in one aggregate are expected to diminish as $l_A - l_B$ decreases. Qualitatively, this seems to be the explanation for the fact that lamellar phase instability has been observed for the $C_{18}K/C_{10}K$ but not for the $C_{18}K/C_{14}K$ system.[24]

IV. CONCLUDING REMARKS

In this paper we have extended our mean-field theory of chain packing in micelles to the important case of mixed chain lengths. This situation is most commonly encountered in real microemulsions and membrane systems, but had not been treated self-consistently by any earlier theories. In order to focus on the effects of conformational free energy, we have considered the case in which the two surfactants have identical head groups. The total free energy per molecule is written as a sum of chain, ("tail") and surface ("head") contributions, with only the former depending on composition; a mixing entropy term is also included.

Before carrying out mean-field calculations for the chain packing, we derived first some simple expressions for the minimum area per molecule in different micellar geometries. These results follow directly from surface/volume relations for the mixed aggregates and represent a generalization of the familiar $a_{\min} = k\mathrm{v}/l$, cf. Eq. (17) where v is the tail volume and l is the fully stretched tail length, and $k = 1$, 2, 3 for bilayers, cylinders, and spheres, respectively. Specifically we establish that—for certain mole fractions of long and short chains—$a_{\min}$ for spheres and cylinders can be significantly lower than in pure micelles. This suggests a coupling between composition and preferred micellar geometry: Similar coupling between composition and curvature fluctuations will have important consequences for splay energies and bending radii at surfactant interfaces.

This idea is confirmed and illustrated by numerical computations of chain conformation statistics. The picture which emerges is one of the long chains being "squeezed" away from the interface in order to fill the inner regime of the hydrophobic core which the short chains cannot reach. Figures 4 and 5 show this for the monomer (segment) density, which is peaked towards the center for the longer molecules. This disordering of the longer tails by the presence of the short ones is also evidenced by the decrease in bond orientational order parameters towards the chain ends (see Figs. 6 and 7) and is confirmed by experiments. Similarly, Figs. 8 and 9 show how the peaks in the terminal group distribution are shifted "inside" (towards the center) as the longer chains are replaced by shorter ones.

Minimization (with respect to area per molecule) of the total free energy, tail plus head plus mixing entropy, shows more explicitly how higher curvatures can be preferentially stabilized by composition changes. Specifically, for discrepant enough chain lengths, a change in mole fraction is found to upset the free energy ordering of bilayer, cylinder, and sphere (see Fig. 12). This result confirms the dominant role played by conformational entropy and helps explain recent experiments in which it is demonstrated that lamellae in mixed fatty acid systems become unstable as soon as the molecules of very different chain lengths reach comparable numbers. Further theoretical work is clearly desirable to understand better the surface (head-group) effects and to treat the case of added alcohol, salt, etc.

ACKNOWLEDGMENTS

The financial support of the US–Israel binational foundation is gratefully acknowledged. The Fritz Haber Molecular Dynamics Research Center is supported by the Minerva Gesellschaft fur die Forschung, Munich FRG. Finally, W.M.G. acknowledges the National Science Foundation (Grant No. CHE-8542620) for its continued financial support.

[1] C. Tanford, *The Hydrophobic Effect*, 2nd ed. (Wiley–Interscience, New York, 1980).
[2] K. M. Jain, *The Bimolecular Lipid Membrane* (Van Nostrand Reinhold, New York, 1972).
[3] See, e.g., (a) *Surfactants in Solution*, edited by K. L. Mittal and P. Botherel (Plenum, New York, 1987); (b) *ibid.* (1984); (c) *Physics of Amphiphiles: Micelles, Vesicles and Microemulsions*, edited by V. Degiorgio and M. Corti (North–Holland, Amsterdam, 1985).
[4] *Phenomena in Mixed Surfactant Systems*, edited by J. F. Scarmehorn, ACS Symp. Ser. (American Chemical Society, Washington, D.C., 1986).
[5] P. Ekwall, Adv. Liq. Cryst. **1**, 1 (1975).
[6] (a) H. Wennerstrom and B. Lindman, Phys. Rep. **52**, 1, (1980); (b) B. Lindman and H. Wennerstrom, Top. Curr. Chem. **87**, 1 (1980).
[7] P. Schurtenberger, N. A. Mazer, and W. Kanzig, J. Phys. Chem. **89**, 1042 (1985).
[8] M. C. Carey and D. M. Small, Man. J. Clin. Inves. **61**, 998 (1978).
[9] D. Lichtenberg, Biochem. Biophys. Acta **821**, 470 (1985).
[10] See, e.g., (a) R. Zana, C. Picot, and R. Duplessix, J. Colloid. Interface Sci. **93**, 43 (1983); (b) J. Almgren and S. Swarup, J. Phys. Chem. **87**, 876 (1983).
[11] (a) A. Ben-Shaul, I. Szleifer, and W. M. Gelbart, J. Chem. Phys. **83**, 3597 (1985); (b) **83**, 3612 (1985); (c) Proc. Natl. Acad. Sci. U.S.A. **81**, 4601 (1984); (d) in Ref. 3(c); (e) in Ref. 3(a).
[12] I. Szleifer, A. Ben-Shaul, and W. M. Gelbart, J. Chem. Phys. **85**, 5345 (1986).
[13] For a recent review see: A. Ben-Shaul and W. M. Gelbart, Annu. Rev. Phys. Chem. **36**, 179 (1985).
[14] J. Seelig and W. Niederberger, Biochemistry **13**, 1585 (1974).
[15] H. Walderhaug, O. Soderman, and P. Stilbs, J. Phys. Chem. **88**, 1655 (1984).
[16] (a) P. van der Ploeg and H. J. C. Berendsen, Mol. Phys. **49**, 233 (1983); (b) O. Edholm, H. J. C. Berendsen, and P. van der Ploeg, Mol. Phys. **48**, 379 (1983).
[17] B. Jonsson, O. Edholm, and O. Teleman, J. Chem. Phys. **85**, 2259 (1986).
[18] M. C. Woods, J. M. Haile, and J. P. O'Connell, J. Phys. Chem. **90**, 1875 (1986).
[19] (a) J. N. Israelachvili, D. J. Mitchell, and B. W. Ninham, J. Chem. Soc. Faraday Trans. 2 **72**, 1525 (1976); (b) J. N. Israelachvili, in Refs. 3(a)

and 3(c); (c) D. J. Mitchell and B. W. Ninham, J. Chem. Soc. Faraday Trans. 2 **77**, 601 (1981).
[20]B. Mely and J. Charvolin, in *Physicochimie des Composes Amphiphile*, edited by P. Perron (CNRS, Paris, 1979).
[21]J. B. Rosenholm, T. Drakenberg, and B. Lindman, J. Colloid Interface Sci. **63**, 538 (1978).
[22]R. J. E. M. de Weerd, J. W. de Haan, L. J. M. van de Ven, M. Achten, and H. M. Buck, J. Phys. Chem. **86**, 2523 (1982)
[23]T. Klason and U. Henriksson, in *Solution Behaviour of Surfactants: Theoretical and Applied Aspects*, edited by K. L. Mittal and E. J. Fendler (Plenum, New York, 1982), Vol. 1, p. 417.
[24]J. Charvolin and B. Mely, Mol. Cryst. Liq. Cryst. **41**, 209 (1978).
[25](a) D. W. R. Gruen, J. Phys. Chem. **89**, 146 (1985); (b) **89**, 153 (1985); (c) Ref. 3(a).
[26]P. J. Missel, N. A. Mazer, G. B. Benedek, C. Y. Young, and M. C. Carey, J. Phys. Chem. **84**, 1044 (1980).
[27]A. Ben-Shaul, D. H. Rorman, G. V. Hartland, and W. M. Gelbart, J. Phys. Chem. **90**, 5277 (1986).
[28]D. W. R. Gruen, Prog. Polym. Sci. **70**, 6 (1985).
[29]B. Cabane, R. Duplessix, and T. Zemb, J. Phys. **46**, 2161 (1985).
[30]J. P. Hansen and I. R. McDonald, *Theory of Simple Liquids* (Academic, New York, 1976).
[31]See, e.g., P. J. Flory, *Statistical Mechanics of Chain Molecules* (Wiley–Interscience, New York, 1969).
[32]See, e.g., T. L. Hill, *Introduction to Statistical Thermodynamics* (Addison Wesley, Reading, MA, 1960).